Nondestructive System for Analyzing Carbon in the Soil

Lucian Wielopolski*
Brookhaven National Lab.
Environmental Sciences Dep.
Upton, NY 11973

George Hendrey
Queens College School of Earth and Environ. Sci.
Flushing, NY 11367

Kurt H. Johnsen
USDA-Forest Service
Southern Research Station
Forestry Sciences Lab.
P.O. Box 12254
Research Triangle Park, NC 27709

Sudeep Mitra
Brookhaven National Lab.
Environmental Sciences Dep.
Upton, NY 11973

Stephen A. Prior
Hugo H. Rogers
H. Allen Torbert
USDA-ARS, National Soil Dynamics Lab.
411 S. Donahue Dr.
Auburn, AL 36832

Carbon is an essential component of life and, in its organic form, plays a pivotal role in the soil's fertility, productivity, and water retention. It is an integral part of the atmospheric–terrestrial C exchange cycle mediated via photosynthesis; furthermore, it emerged recently as a new trading commodity, i.e., "carbon credits." When carefully manipulated, C sequestration by the soil could balance and mitigate anthropogenic CO_2 emissions into the atmosphere that are believed to contribute to global warming. The pressing need for assessing the soil's C stocks at local, regional, and global scales, now in the forefront of much research, is considerably hindered by the problems besetting dry-combustion chemical analyses, even with state-of-the-art procedures. To overcome these issues, we developed a new method based on gamma-ray spectroscopy induced by inelastic neutron scattering (INS). The INS method is an in situ, nondestructive, multielemental technique that can be used in stationary or continuous-scanning modes of operation. The results from data acquired from an investigated soil mass of a few hundred kilograms to an approximate depth of 30 cm are reported immediately. Our initial experiments have demonstrated the feasibility of our proposed approach; we obtained a linear response with C concentration and a detection limit between 0.5 and 1% C by weight.

Abbreviations: INS, inelastic neutron scattering; LIBS, laser-induced breakdown spectroscopy; MDL, minimum detectable limit; NG, neutron generator; TNC, thermal neutron capture.

Maintaining and increasing the organic matter in soils adds to its fertility and retention of water, and, hence, increases crop production. Carbon transport and retention in soil also is an integral part of the atmospheric–terrestrial C-exchange cycle mediated via photosynthesis. It was recognized that the terrestrial sequestration of C plays an important mitigating role in moderating the rise in global temperature thought to be caused by anthropogenic greenhouse gases that trap heat in the atmosphere and ultimately lead to changes in global climate patterns (Hasselmann, 1997). The rate of such change expected during the next 100 yr will be unprecedented in human history. Since the beginning of the 20th century, the mean surface temperature of the earth has increased by about 0.5°C (about 1.0°F). There is strong evidence that most of the warming during the last 50 yr is due to human activities that have altered the chemical composition of the atmosphere through the buildup of greenhouse gases, in particular by adding large amounts of CO_2 (United Nations Environment Programme, 2003, p. 3–7). The dramatic increase in atmospheric CO_2 concentrations from approximately 0.025% (w/w) in the pre-Industrial Revolution period, to about 0.036% (w/w) at present (Lal et al., 1998) is at the center of the climate debate about global warming. The main sources of CO_2 emissions are attributed to burning fossil fuels and biomass, and to changes in land use, deforestation, and soil-management practices (Bhatti et al., 2006). Less than half of the emissions has remained in the

Soil Sci. Soc. Am. J. 72:1269-1277
doi:10.2136/sssaj2007.0177
Received 15 May 2007.
*Corresponding author (lwielo@bnl.gov).

atmosphere, however. The other half has been taken up and stored as organic matter in vegetation, soils, and river basins on land, and in the sea as sediments or dissolved CO_2 (Wofsy and Harriss, 2002; Climate Change Science Program, 2003). On land, these extensive emissions are partially mitigated by the temporary sequestering of C in the soil through photosynthetic processes and no-till agricultural practices.

With its integral role in the C cycle, soil contains a huge dynamic pool of C that is a critical regulator of the global C budget. As the repository for three-fourths of the earth's terrestrial C, soils store 2.5 times the amount contained in vegetation. Terrestrial ecosystems, the vegetation and soils containing microbial and invertebrate communities, are huge natural biological scrubbers of atmospheric CO_2, sequestering directly from the atmosphere about 25% ($\sim$2 Pg C yr^{-1}) of the 7.4 Pg C emitted annually by human activities and storing it as soil organic C (SOC). The dynamics of SOC are governed by factors such as variations in photosynthates, the C content of plant roots, and plant litter on the soil's surface. Much of the basic biological understanding that is taken for granted in aboveground ecosystems, however, is lacking belowground; indeed, the identification and quantification of belowground biota, food webs, and their functional implications for the ecosystem lag far behind aboveground systems. Furthermore, knowledge of the soil processes in agricultural systems is much more advanced than it is for unmanaged soils.

Restoring C in soil is essential to enhancing its quality, sustaining and improving food production, and improving water retention. Increasing C sequestration in soil by proper management practices was vigorously proposed as a means for mitigating the atmospheric buildup of CO_2 (Lal et al., 2004). Thus, accurately determining the C in soil is vital to enhancing its quality and fertility, and also more and more important in meeting society's emerging need to broker C sequestration via soil C credits under the U.S. Department of Energy's Voluntary Greenhouse Gas Reporting Program, established by Section 1605(b) of the Energy Policy Act of 1992. In addition, quantifying the resulting changes in the soil's C stocks is essential for evaluating and documenting the value of any schemes for mitigation. Belowground studies pose special challenges because the structures, organisms, and processes there are invisible from the soil's surface. The satellite remote sensors that have advanced aboveground C studies are useless as they do not penetrate below the ground surface. Therefore, there is a pressing need for better technologies for in situ C monitoring that are nondestructive, quantitative, and can operate in either static or dynamic modes for scanning large land areas (Johnston et al., 2004). Established methods of quantifying C in soils by core sampling are destructive, labor intensive, and their scope is limited. New technologies must be cheaper, support rapid analyses, and enable repetitive, nondestructive, sequential measurements.

Several analytical technologies have emerged recently that greatly advance the capability for analyzing soil samples, generating a wealth of information surpassing that of conventional dry-combustion analysis (Wielopolski, 2006). One such technique is soil pyrolysis coupled with molecular-beam mass spectrometry. This laboratory technique, which requires sample preparation, characterizes the SOC chemical components by rapid pyrolysis, "freezing" the low-molecular-weight fragments in a molecular beam that is sent to a mass spectrometer for analysis. The fragments' mass spectra (10–500 Da) are chemically rich and retain information about their parental complex molecules (Evans et al., 1984; Magrini et al., 2002).

A second method, near-infrared and mid-infrared diffuse reflectance spectroscopy (NIR), is based on the specific molecular vibrations caused when samples are exposed to infrared radiation. Comparing the acquired spectra to the spectrum of incident light reveals the type and quantity of specific molecules in the sample. These spectra are evaluated with a complex principal component analysis statistical package that derives the most significant components in the spectrum and subsequently relates them to C concentration. Several laboratories use NIR for quantitative soil analysis (Chang et al., 2001; Ehsani et al., 1999; Fystro, 2002; McCarty et al., 2002; Reeves et al., 1999; Shepherd and Walsh, 2002; Viscarra Rossel et al., 2005). With minimal sample preparation, NIR measurements provide very localized results. Two NIR systems were developed recently to measure diffuse reflectance through a sapphire window in direct contact with the soil. One, a shank equipped with a NIR system, cuts through the soil at a given depth and analyzes the material within about a distance of 1 cm from the shank; in the second, a NIR system is mounted on a vertical probe to penetrate the soil vertically.

In a third method, laser-induced breakdown spectroscopy (LIBS), a laser focused on a soil sample vaporizes about a 10 μL volume, forming ionized plasma, i.e., ionized gas. As the sample cools, the plasma electrons recombine with the ionized molecules and atoms, emitting concomitant light that is collected via fiber optics and spectrally resolved. The acquired spectra are analyzed for matrix effects and elements via their spectral signatures (Cramers et al., 2001; Kincade, 2003; Mouget et al., 2003; Ebinger et al., 2003).

Finally, under a different, noninstrumental approach, C-Lock software evaluates the accrual of C in soil based on information about the site and the agricultural management practices; it then quickly generates estimates of standardized C-emission reduction credits. Although this methodology is being used, it requires verification procedures.

Although the methods we have described are more advantageous than the dry-combustion laboratory analysis of soil, they are destructive, provide point measurements only, and most require core samples. Another indirect method of assessing C in soil, which is widely used for estimating global stocks, is based on readings from AmeriFlux Network towers (Goulden et al., 1996; Frolking et al., 1996; Curtis et al., 2002), wherein the C balance in soil is assessed from the difference in the upward and downward atmospheric CO_2 fluxes; this difference reflects the gain or loss of C in the soil. These are stationary systems, however, affording local values.

Despite the importance of C in the belowground processes that we have outlined, C monitoring could greatly benefit from having better analytical tools for nondestructive soil C analysis. Taking soil cores to analyze C interferes with the very processes that we are measuring. Compounding this problem is the considerable effort and cost involved in current sampling and analysis methodologies. Our new instrument for in situ nondestructive measurement of C and other elements present in soil elimi-

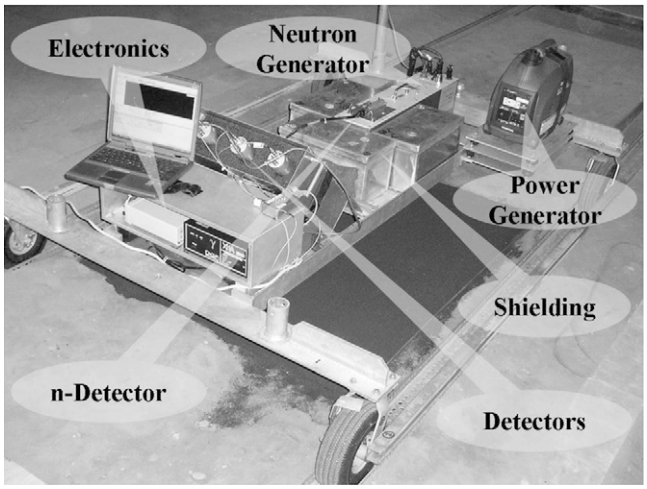

Fig. 1. Inelastic neutron scattering alpha prototype, with major components identified, placed above a synthetic soil pit.

nates these drawbacks. The instrument, based on spectroscopy of gamma rays stimulated by fast and slow neutrons interacting with the soil elements, can be used in stationary and continuously scanning modes. We demonstrate here the feasibility of using high-energy neutrons and photons to sample soil volumes up to about 0.3 m^3 and approximately 20 to 30 cm deep, with a 150-cm-diameter footprint (Wielopolski et al., 2004).

MATERIALS AND METHODS

Inelastic Neutron Scattering System

The new INS system is comprised of a neutron generator (NG) embedded in and surrounded by shielding, an array of NaI detectors, electronics for nuclear spectroscopy, and a plastic neutron detector. Figure 1 illustrates an alpha prototype of the INS system, with its main components identified. The fast, 14 MeV, neutrons are produced in a miniature (2.5 cm in diameter and 10 cm long) sealed-tube accelerator in which a deuterium beam impinges on a titanium target impregnated with tritium. The resulting (d,t) fusion reaction emits an isotropic α particle with a concomitant antiparallel fast neutron (Csikai, 1987). A fraction of the emitted fast neutrons interact with the soil elements, inducing emission of characteristic gamma rays. The three principal neutron interactions with matter are: (i) inelastic neutron scattering (n,n′,γ) by which fast neutrons, above some threshold energy, are captured by a nucleus and reemitted at lower energy with concurrent emission of prompt gamma rays characterizing the INS spectrum, e.g. in soil, Si (1.78 MeV), C (4.43 MeV), and O (6.13 MeV); (ii) elastic neutron scattering wherein fast neutrons collide elastically with the nuclei in the soil matrix and slow down, losing kinetic energy until they become thermal (in thermal equilibrium with the surroundings)—H atoms are the ones that cause the loss of the most energy per scattering; and (iii) thermal neutron capture (n,γ) in which a thermal neutron is captured by a nucleus, stimulating the emission of prompt gamma rays. The thermal neutron capture (TNC) spectrum is best suited for the determination of N and P. Very often (n,γ) reactions result in the formation of a radionuclide, which may also emit gamma rays during decay. Delayed gamma measurements can be used to determine Cl, Na, and Ca; however, these spectra were not measured in this study (Evans, 1955; Alfassi and Chung, 1995; Chrien and Kane, 1979; Nargolwalla and Przybylowicz, 1973). Since the INS and TNC events are separated by a thermalization time of about several hundred microseconds, we can gate the system using a

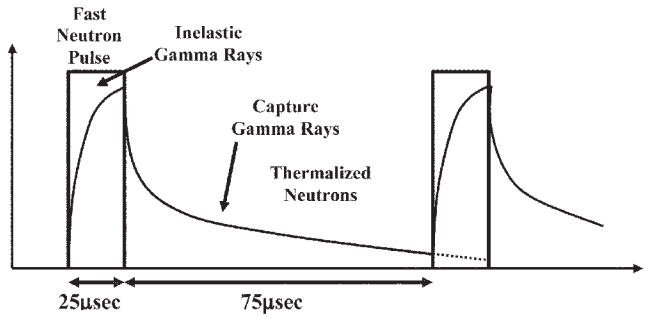

Fig. 2. Pulsing sequence of the neutron generator.

pulsed NG, and concurrently acquire separate INS and TNC spectra, thus reducing the background in each of them. In this study, we operated the NG at a repetition rate of 10 kHz and duty cycle of 25%; thus, the INS spectra were acquired during the 25-μs duration of the neutron pulse, and the TNC spectra during the remaining 75 μs between the neutron pulses. Figure 2 shows the pulsing sequence. At the same time, the neutron output of the NG was monitored with a plastic scintillator. In the alpha prototype system, the stimulated gamma rays were detected by an array of three NaI(Tl) scintillation detectors, then digitally processed and stored as frequency histograms or pulse-height distributions; Fig. 3 depicts a typical INS and a TNC spectrum. The spectral peak intensities (net areas) are proportional to the number of atoms of interest present in the interrogated volume that is defined by the intercept of the neutron field and the solid angle subtended by the detection system, and the counting time. The initial feasibility demonstration of the system was reported by Wielopolski et al. (2000). We emphasize that since the NG is an electrical device, it can be

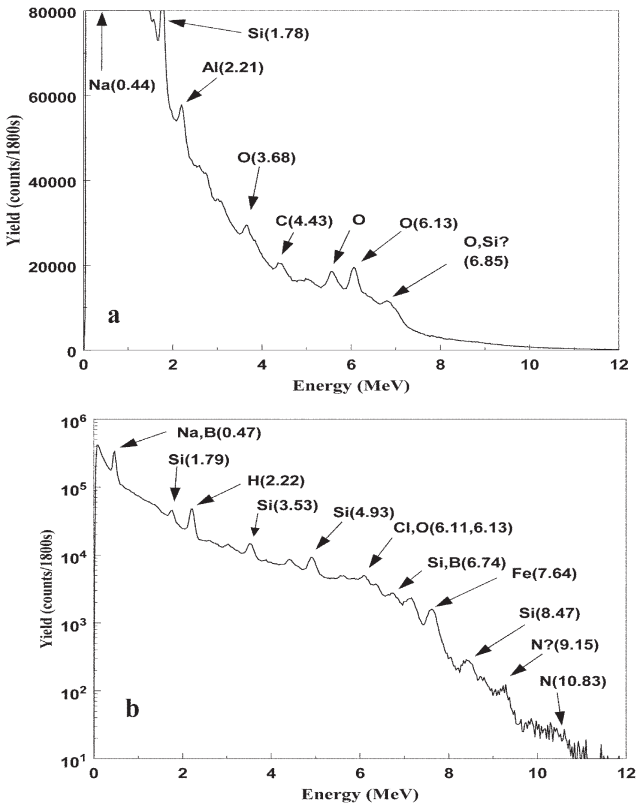

Fig. 3. (a) An inelastic neutron scattering spectrum, and (b) a thermal neutron capture spectrum, acquired concurrently in a pine stand during 30 min.

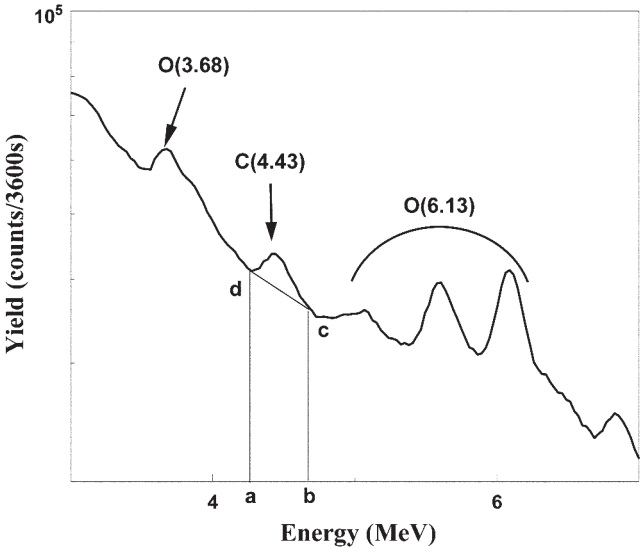

Fig. 4. The calculation of the net C peak area is the total area between *a* and *b*, minus the area defined by the trapezoid *abcd*.

switched off, stopping any neutron production, in stark contrast to gauges using radioactive neutron sources that emit neutrons continuously.

Spectral Analysis

There are several methods for analyzing gamma ray spectra. The simplest, trapezoidal method, depicted in Fig. 4, consists of evaluating the net peak area, N_p, in the region of interest as a difference between the total area, T, between the a and b markers in Fig. 4 and the background area, B, bound by the trapezoid abcd. For low-intensity peaks in NaI gamma ray spectra, the background under the peak, to the first approximation, can be assumed to be linear. There are more advanced spectra analysis methods, however. Thus, when no interferences are present we can write

$$N_p = T - B \quad [1]$$

The uncertainty in Eq. [1] results from errors in T and B that are associated with nuclear counting, as represented by Poisson's statistics, and for large numbers they are approximated by $\sqrt{T}$ and $\sqrt{B}$. Thus, we can propagate the uncertainty for the net number of counts (σ_{Np}) as

$$\sigma_{N_p} = \sqrt{T + B} \quad [2]$$

Two fundamental quantities of the INS system that define its performance are sensitivity, s, and background, B, defined as the net number of counts per gram of material C acquired per unit time, t, per neutron, n (net counts g^{-1} s^{-1} $neutron^{-1}$)

$$s = N_p / Ctn \quad [3]$$

This relationship between spectral counts and material abundance is derived during the calibration procedure, and the background is obtained from measured spectra as the trapezoidal area.

These equations demonstrate that the signal is proportional to the counting time, t, whereas the uncertainty is proportional to the square root of the acquisition time, resulting in relative decreases in uncertainty as the counting time increases. The minimum detectable limit (MDL) is defined as the change in the background counts that will indicate the presence of a peak with a given confidence level. For example, at the 99% confidence level, the MDL = $3\sqrt{B}$. Similarly, we define minimum detectable change (MDC) as a change in the net number of counts, MDC = $3\sigma_{Np}$. Therefore, any optimization of an INS system focuses on reducing the background and increasing the system's sensitivity.

The net number of counts in the C 4.44-MeV photopeak, N_p, must be corrected to account for two interferences, however, and so give the true number of counts due to C, N_C. The first interference reflects thermal neutron captures in a ^{28}Si yielding 4.94-MeV gamma rays that interact in a NaI detector generating a single escape peak (SEP) at 4.94 – 0.511 = 4.43 MeV. By and large, this peak occurs in the TNC spectrum; however, this depends on the NG's pulsing regimen and on the lifetimes of the INS and TNC data acquisition times, LT_{INS} and LT_{TNC}, respectively (Mitra and Wielopolski, 2005). The SEP interference's contribution to the C peak counts, C_{SEP}, is

$$C_{SEP} = \mathrm{Si}(4.43)\,\mathrm{LT}_{INS}/\mathrm{LT}_{TNC} \quad [4]$$

The second interference is due to nuclear excitations of ^{28}Si in which the excited nucleus decays to the ground state via many cascades (CASs) feeding down to the 1.78-MeV level, which decays to the ground state. A fraction of the cascade originates at the 6.23-MeV level, generating 6.23 – 1.78 = 4.45 MeV gamma rays (C_{CAS}) that overlap with the C peak. We note that the 1.78-MeV Si peak itself must be corrected for $^{28}Si(n,p)^{28}Al$ reactions that, with a 2.25-min half-life also contribute to the 1.78-MeV line. Since all the interferences are associated with peaks that are acquired concurrently with the C peak, the corrections are implemented for each individually measured spectrum by Eq. [4] and

$$C_{CAS} = \left[\mathrm{Si}(1.78) - \mathrm{Al}(1.78)\,\mathrm{LT}_{INS}/\mathrm{LT}_{TNC}\right]0.0547 \quad [5]$$

The constant factor 0.0547 is a theoretical value based on calculated production and decay cross-sections using EMPIRE, a modular system of nuclear reaction codes (Herman et al., 2007). The errors associated with these theoretically and experimentally determined correction factors are estimated at about 10%. Thus, the number of counts in the C peak due to C, N_C, is

$$N_C = N_p - C_{SEP} - C_{CAS} \quad [6]$$

System Calibration

The INS system initially was calibrated with synthetic soils consisting of uniform mixtures of clean sand with granular C, from Calgon Carbon Corp. (Pittsburgh, PA), at 0, 2.5, 5, and 10% (w/w). The mixtures, each weighing about 1590 kg, were placed in a 115- by 144- by 45-cm^3 pit and C spectra were acquired with a single detector placed on the top of the pit for 30 min. Each measurement was repeated four times and the acquired spectra were analyzed for C, Si, and O peaks. Since the C signal is proportional to the total number of C atoms in the interrogated volume, the INS system could be calibrated against C density, ρ_c (g C cm^{-3}), as derived by multiplying the nominal C-weight fraction by the soil's measured bulk density determined for every C mixture. For an arbitrary C profile, however, which generally is not homogeneous, a more appropriate quantity to use is the projection of the volumetric C onto the soil's surface, C_s (g C cm^{-2}), i.e., the total C contained under the system's footprint. Thus, the system was calibrated in terms of C yield vs. surface C den-

sity obtained by multiplying the C density by a constant depth of 30 cm. Table 1 summarizes the raw C yields and those corrected for Si interferences using Eq. [5], together with the soils' bulk densities in the homogenous synthetic soils. The calibration lines for the raw data and the corrected yield are plotted in Fig. 5a and 5b, respectively. The slopes of these lines represent the sensitivity *s* of the system with one detector on the ground and an 1800-s counting time. Improving the system by placing three detectors 30 cm above the ground, referred to hereafter as the INS alpha prototype, improved the sensitivity by about a factor of 4.1.

Table 1. Carbon calibration using synthetic soil in a sand pit for four homogeneous C concentrations in sand to a depth of 30 cm (standard deviations in parentheses).

C content of sand	Bulk density	C concentration	C surface concentration	C yield	C yield corrected
% (w/w)	g cm^{-3}	g C cm^{-3}	g C cm^{-2}	—— counts ——	
0.0	1.53 (10)	0	0	5305 (9.2)	0 (6.4)
2.5	1.50 (10)	0.037	1.125	7331 (1.6)	1976 (1.3)
5.0	1.44 (10)	0.073	2.160	10614 (4.2)	4252 (4.8)
10.0	1.40 (10)	0.140	4.200	15545 (1.4)	9408 (6.7)

The response function of the INS system, INS_{RF}, i.e., the number of counts in the C peak, can be expressed analytically as a multiple space-, time-, and energy-dependent integral given by

$$INS_{RF} = \int_0^T dt \int_{-\infty}^{\infty} dx \int_{-\infty}^{\infty} dy \int_0^{\infty} dz \int_{E_{th}}^{14} dE \phi_n(x,y,z,E) EL(x,y,z) \sigma(E) \times C_C(x,y,z) D_b(x,y,z) \Omega(x,y,z) A_{att}(x,y,z) Det_g(x',y',z',E_g) \quad [7]$$

This integral cannot be solved analytically and any numerical procedure will be very cumbersome; instead, it can be assessed using a Monte Carlo probabilistic simulation (Wielopolski et al., 2005). The various components in Eq. [7] include the following: $\phi_n(x,y,z,E)$, the energy-dependent neutron flux at position *x*,*y*,*z* in the soil; EL(*x*,*y*,*z*), the soil's elemental composition; $\sigma(E)$, the energy-dependent cross-sections for neutron interaction with the matrix elements; $C_c(x,y,z)$, the C-profile distribution; $D_b(x,y,z)$, the soil's bulk density; $\Omega(x,y,z)$, the solid angle subtended by the detection system from the point of C gamma ray production; A_{att}, the attenuation of the gamma ray from its point of production to the detection system; and $Det_g(x',y',z')$ the detector's response function to the incident gamma ray radiation. We note that the primed coordinates refer to the detection system's dimensions. Excluding the detector's response function, the Monte Carlo simulation of the INS system is denoted in Fig. 5 by circles. The simulation depicted was normalized to an experiment with the highest C concentration in a soil volume of 250 by 200 by 50 cm deep.

RESULTS

We initially demonstrated the viability of the INS system for measurements in the field at Brookhaven National Laboratory using a single detector system placed on the ground. After basic improvements, we used three detectors, elevated about 30 cm above the ground; this system, referred to as the alpha prototype, underwent field tests at Duke Forest, Durham, NC. Following nondestructive INS measurements there, samples of soil were taken from the same spots and subjected to standard chemical analysis by independent researchers.

Studies at Brookhaven National Laboratory

Three sites, a pitch pine (*Pinus rigida* Mill.) stand, a sandy patch filled with plant debris, and a scrub oak (*Quercus ilicifolia* Wangenh.) forest were selected for soil C analysis. At first, INS measurements were acquired for 30 min, and then five soil cores, each 5 cm in diameter, were collected, one in each corner of a 30-cm square (0.09 m^2) and one in the center, representing the approximate footprint of the INS system. The 40-cm-long cores were partitioned into increments of 0 to 5, 5 to 10, 10 to 20, 20 to 30, and 30 to 40 cm; they were prepared for analysis of soil bulk density and moisture determination following standard procedures (Dane and Topp, 2002, Ch. 2 and 3, respectively); these results are summarized in Tables 2 and 3. After sieving (<2 mm) and homogenizing the sample, two 1-g aliquots of soil were taken from each increment, dried at 55°C, ground to pass through a 0.15-mm sieve, and analyzed for total C using conventional dry-combustion chemistry. A LECO CN 2000 furnace (LECO Corp., Saint Joseph, MI) was operated at a combustion temperature of 1350°C. The results of the C analysis, reported as percentage C by weight, are summarized in Table 4 as mean values of the duplicate aliquots from each increment. The large variations in the individual values in Tables 3, 4, and 5 and the resulting variability in the mean values are quite apparent. The variations in the soil's bulk density combined with those in the C-density profile (Fig. 6) yielded the calibration line in Fig. 7, which differed from that derived for the homogeneous soil. These effects increased the sensitivity of the INS system because C concentrations were higher closer to the surface; the regression-line statistics are summarized in Table 5. The two calibration lines in Fig. 7 show again the regression lines before and after correcting for Si interference.

Duke Forest Studies

At Duke Forest, measurements were taken with the alpha prototype instrument from three sites. All sites are adjacent to each other in the Blackwood Division of the Duke Forest near Durham, NC (35°58′41.430″ N, 79°5′39.087″ W). The pine site was planted in 1993 with loblolly pine (*Pinus taeda* L.) and has not been managed since establishment. The hardwood site is an uneven-aged, 80- to 100-yr-old oak (*Quercus* spp.)–hickory (*Carya* spp.) forest, also not managed since establishment. The grassland is dominated by the C_3 grass *Festuca arundinacea*

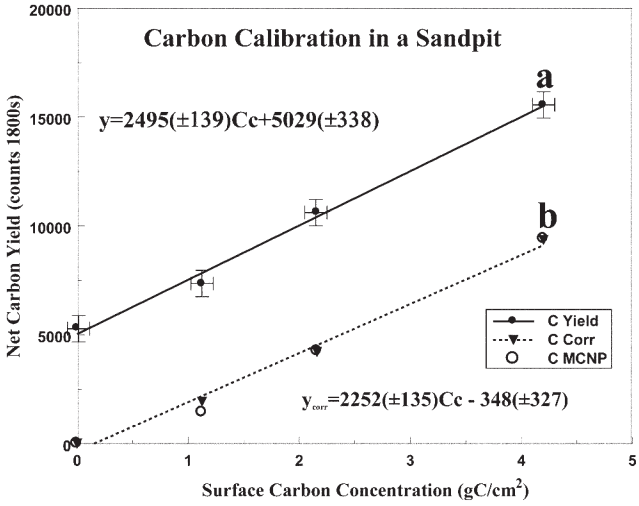

Fig. 5. Calibration line least-squares fit of the net C yield vs. C concentration in the sand pit.

Table 2. Total moisture content of every core section obtained by weighing before and after drying. All measured at Brookhaven National Laboratory.

Depth	Core 1	Core 2	Core 3	Core 4	Core 5	Mean ± SD
cm	g					
			Pine stand			
0.0–5.0	8.32	7.44	13.03	10.19	7.81	9.36 ± 2.3
5.0–10	4.39	5.41	7.59	5.06	5.54	5.60 ± 1.2
10–20	11.43	11.96	11.53	11.03	11.11	11.42 ± 0.4
20–30	11.81	10.99	11.91	10.08	11.03	11.16 ± 0.7
30–40	11.08	11.29	12.60	10.14	11.19	11.26 ± 0.9
			Sandy patch			
0.0–5.0	6.20	6.19	4.91	5.61	5.24	5.63 ± 0.6
5.0–10	5.97	5.22	5.02	5.23	4.22	5.13 ± 0.6
10–20	9.34	9.59	10.64	10.39	10.43	10.28 ± 0.6
20–30	14.79	13.95	12.76	15.25	15.38	14.43 ± 1.1
30–40	15.96	17.69	18.19	19.01	16.60	17.49 ± 1.2
			Oak forest			
0.0–5.0	15.13	11.79	14.46	10.61	12.72	12.94 ± 1.9
5.0–10	9.79	8.80	9.53	8.5	9.41	9.21 ± 0.5
10–20	19.75	21.31	20.87	19.21	21.18	20.46 ± 0.9
20–30	23.56	24.17	22.67	20.15	20.03	22.12 ± 1.9
30–40	26.15	24.67	21.71	20.17	22.56	23.05 ± 2.4

Schreb., with minor forb and C_3 and C_4 grass species and is mowed at least once annually for hay. More details on the sites can be found in Stoy et al. (2006).

The soil at Duke Forest is generally classified as an Enon silt loam, a low-fertility fine, mixed, active, thermic Ultic Hapludalf, typical of the southeastern U.S. Piedmont. The gamma-ray spectra were acquired for 30 min, after which 2.5-cm-diameter cores were collected to measure the soil's moisture content. In addition, excavation pits 40 by 40 by 40 cm^3 in layers of 5, 5, 10, 10, and 10 cm thick were taken from the measurement sites for C analysis and assessments of the solid and woody fractions. Three large samples from each layer were cleaned and homogenized, and two 1-g aliquots (subsamples) underwent combustion analysis for C. During the INS measurements, the fields were about 100% water saturated, 20 to 50% by weight, and their rocky coarse fragment content (>2 mm) varied between 5 and 30% by weight.

Table 3. Bulk density of every core section obtained by dividing the dry weight by the volume.

Depth	Core 1	Core 2	Core 3	Core 4	Core 5	Mean ± SD
cm	g cm^{-3}					
			Pine stand			
0.0–5.0	1.11	1.01	0.85	0.64	1.01	0.92 ± 0.18
5.0–10	0.92	1.14	1.25	1.00	1.21	1.10 ± 0.14
10–20	1.42	1.31	1.47	1.23	1.40	1.37 ± 0.10
20–30	1.45	1.54	1.53	1.34	1.42	1.46 ± 0.08
30–40	1.52	1.49	1.52	1.35	1.34	1.44 ± 0.09
			Sandy patch			
0.0–5.0	1.93	1.87	1.85	2.02	2.09	1.95 ± 0.10
5.0–10	1.92	1.81	1.89	2.00	1.86	1.90 ± 0.07
10–20	2.11	2.08	2.09	2.07	2.11	2.09 ± 0.02
20–30	2.08	2.01	2.12	1.91	2.07	2.04 ± 0.08
30–40	1.92	1.90	1.95	2.00	2.07	1.97 ± 0.09
			Oak forest			
0.0–5.0	0.40	0.86	0.52	0.62	0.62	0.61 ± 0.17
5.0–10	1.17	1.09	1.09	1.13	1.09	1.11 ± 0.04
10–20	1.30	1.50	1.36	1.45	1.36	1.39 ± 0.08
20–30	1.49	1.40	1.47	1.52	1.36	1.45 ± 0.07
30–40	1.48	1.51	1.58	1.48	1.42	1.50 ± 0.06

Table 4. Mean values of C analysis of two aliquots taken from each core section.

Depth	Core 1	Core 2	Core 3	Core 4	Core 5	Mean ± SD
cm	% C (w/w)					
			Pine stand			
0.0–5.0	5.03	5.07	10.81	15.12	6.74	8.55 ± 4.40
5.0–10	1.96	2.00	2.71	2.36	1.93	2.19 ± 0.33
10–20	1.22	1.56	1.28	1.97	1.15	1.44 ± 0.34
20–30	0.79	0.79	1.03	0.93	1.07	0.92 ± 0.13
30–40	0.43	0.70	1.15	0.67	0.77	0.74 ± 0.26
			Sandy patch			
0.0–5.0	1.17	1.37	1.36	1.20	1.27	1.27 ± 0.09
5.0–10	0.94	0.69	0.86	0.85	0.83	0.83 ± 0.09
10–20	0.44	0.41	0.51	0.34	0.37	0.41 ± 0.07
20–30	0.48	0.54	0.33	0.81	0.49	0.53 ± 0.17
30–40	0.39	0.45	0.49	0.38	0.28	0.40 ± 0.08
			Oak forest			
0.0–5.0	26.90	8.18	17.65	10.71	14.00	15.5 ± 7.30
5.0–10	1.66	1.99	2.35	2.44	2.35	2.16 ± 0.33
10–20	0.78	0.89	0.91	0.98	1.20	0.95 ± 0.16
20–30	0.52	1.79	0.74	0.73	0.54	0.86 ± 0.53
30–40	0.45	0.79	0.34	0.59	0.52	0.54 ± 0.17

Figure 8 shows the nine points from the three regions that were jointly used for calibrating the INS system against C analysis by dry combustion; the 95% confidence interval hyperbolas are included. Due to the restricted number of calibration points, a basic test of validity of the calibration line was made using the jack-knifing method in which a new calibration line is fitted to a subset of eight points, and the ninth one is predicted from the new calibration. Repeating this for the nine individual points, the predicted values were compared with the measured ones and plotted in Fig. 9 together with the 1:1 line. The regression line was also determined using a bootstrapping method in which a set of nine points were resampled with returns to create an alternative n sets of nine points for which n new regression lines were calculated. We evaluated the distribution of the regression r values for n = 5000 with the various confidence levels around the maximum likelihood estimation of the r value (not shown). This distribution was positively skewed, and, at a 50% confidence level, all the r values were completely positive, thus indicating an overall positive correlation between these two methods of C analysis in soil. The distributions of the slopes a and the intercepts b also were positively correlated, but were narrower than that of the r val-

Table 5. The sensitivities (slopes) and the intercepts of the regression lines for various studies.

Site	Slope	Intercept	Regression r
	counts kg^{-1} C m^{-2} h^{-1}		
Sand pit	45,040 ± 2,700	−696 ± 654	0.996
Brookhaven Forest	187,360 ± 6,800	−4664 ± 474	0.999
Duke Forest	647,540 ± 66,820	−8450 ± 3806	0.965

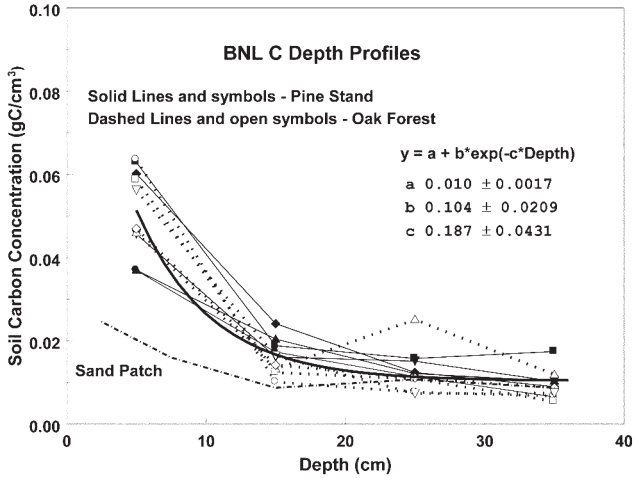

Fig. 6. Individual Brookhaven National Laboratory (BNL) C depth profiles in the pine stand and oak forest. The former is shown as a single separate line. The thick line is the nonlinear fit to all data points.

ues. Thus, although the number of points is very limited, these two methods of C analysis closely correspond.

Carbon Depth Profiles

Since INS measures large volumes to an approximate depth of 30 cm, it was important to assess the C-depth profile. Those obtained in experiments at Brookhaven (Fig. 6) are similar to those measured from nine spots in Duke Forest (Fig. 10). In each case, the thick solid lines in the graphs represent a C transport model given by Eq. [8] that was fitted using nonlinear least squares. The fitted function is

$$C_C = a + b\exp(-cz),\ \text{g C cm}^{-3} \qquad [8]$$

where C_C is the C concentration (g C cm^{-3}) and z is depth (cm). The parameter a (g C cm^{-3}) represents the steady-state background signal, possibly due to inorganic C, whereas the parameters b and c represent the dynamic part of the C profile. The parameter b is the initial surface C level (g C cm^{-3}), while c is the C distribution constant (cm^{-1}), which may vary from soil to soil and represents the steepness of the C profile.

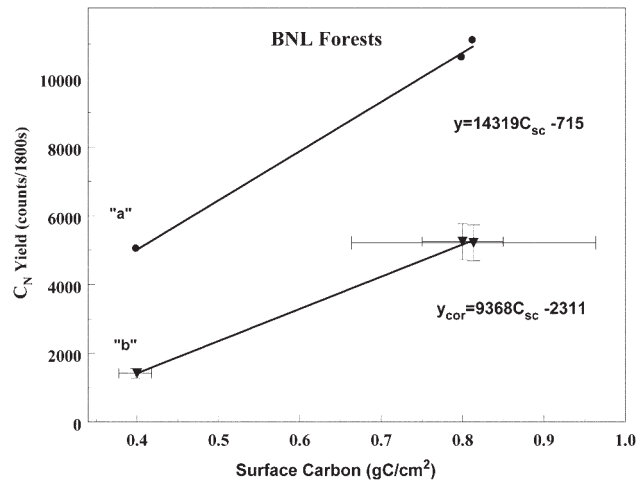

Fig. 7. Brookhaven National Laboratory (BNL) field calibration lines to all data points: Line a is raw data; Line b is interference-free data.

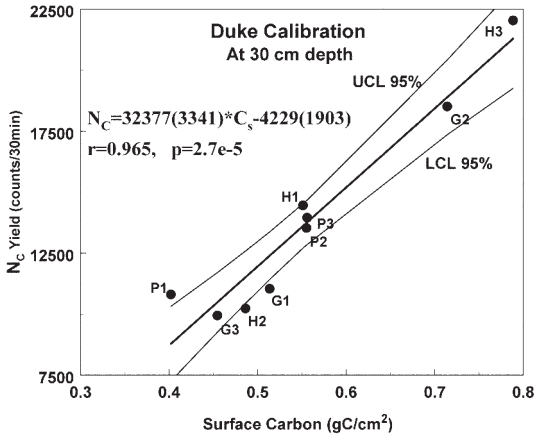

Fig. 8. Carbon calibration, with 95% confidence intervals, in Duke Forest using all field points from the grass, pine forest, and hardwood forest areas; N_C is the number of counts due to C.

Integrating Eq. [8] from a depth A to a depth B, where A is usually zero at the surface and B is 30 cm belowground, yields the surface C density C_s, Eq. [9] (g C cm^{-2}), representing the projection of a belowground C onto surface unit area

$$C_s = az - (b/c)\exp(-cz)\Big|_A^B,\ \text{g C cm}^{-2} \qquad [9]$$

The results of Eq. [9], together with the measured values for Brookhaven and Duke Forest, are summarized in Table 6; for both sites, there is ~5% difference between the integrated and mean measured values.

DISCUSSION

The ever-escalating demands for elemental soil analysis, in particular for soil C analysis, in a variety of research and land- and soil-management efforts dealing with global warming, land disturbances, wetlands, permafrost, precision agriculture, remote monitoring, upscaling, and site monitoring for C credits, have surpassed the natural limitations of conventional chemical analysis by dry combustion. Since the dry-combustion method is time consuming, labor intensive, and destructive and provides only a point measurement in time

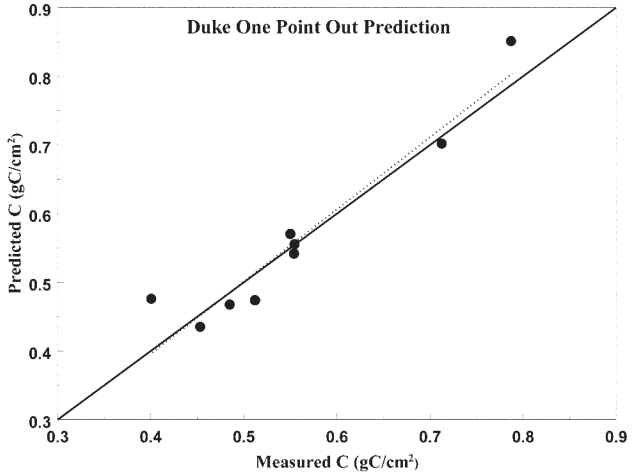

Fig. 9. Predictions of jack-knifing calibration vs. measured values in Duke Forest. The regression dotted line is very close to the solid identity line.

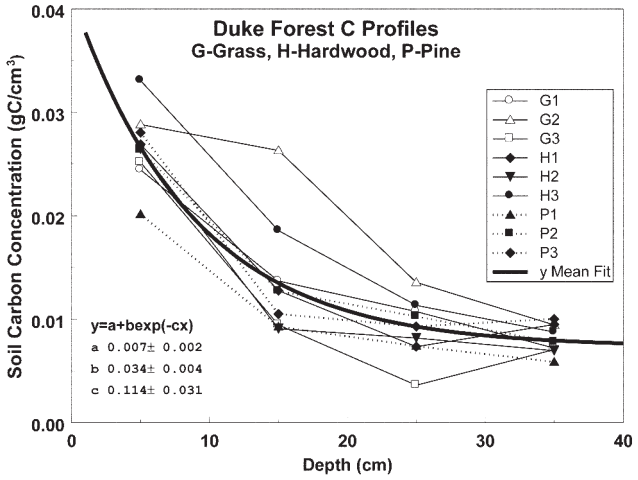

Fig. 10. Carbon depth profiles derived from Duke Forest excavations. The thick line represents the nonlinear fit to all data points.

and space, it cannot yield truly sequential results covering large numbers of samples collected from large areas. These limitations have been partly remedied by the emergence of advanced analytical modalities employing infrared radiation, laser ablation, and nuclear physics principles. These modalities, however, are vastly different in their physical characteristics, performance, and data analysis procedures so that optimizing their utilization necessitates a detailed description of what is being measured and how, together with the data analysis procedures. No single instrument can address all the outstanding issues.

In this study, we outlined the basic nuclear principles of the INS method to measure elemental C in soil, which is independent of the C's chemical configuration. Using synthetic soils, we demonstrated the linearity of the C signal with concentration in the soil, and described our analyses of the spectral signal with error propagation, stipulating the high specificity of the measurement to C. This contrasts with implementing principal component analysis in which any specificity is lost and there is rejection (smoothing) of data points due to selecting a finite number of principal components. Two interferences with the C peak were identified from neutron interactions with Si, namely escape peak and a cascade, and corrected using concurrently measured Si peaks.

Because of the multiplicity of steps involved in the dry-combustion method, i.e., sampling the soil, preparing the samples, and analyzing the samples, there is extensive error propagation that is inseparable from the natural variability in the soil's parameters. For example, as shown in Table 2, the uncertainty or variability in soil moisture in the mean values of five cores varies from about 25% near the surface and decreases with depth. Similarly, the reported near-surface bulk density entails an uncertainty of 25%, which decreases with depth. Since the dry-combustion method always determines C percentage by weight, however, the values of the near- surface bulk density are critical for determining the C stocks. This is not an issue for INS measurements since it is an in situ method calibrated in terms of grams of C per square centimeter. Moreover, for similar reasons, the effect of soil compaction resulting from a change in soil management from tillage to no-till is considerably less when using the INS system to evaluate the soil's C content. As listed in Table 4, the reported C content in the top 5-cm layer carries about a 50% error. Such errors lower the MDL for C and, consequently, the ability to measure changes with time in C stocks; this C MDL should not be confused with the instrumental MDL, which might be very good in the milligram per kilogram range but is lost in the procedures required for analyzing the samples and back-projecting to the field level. These steps do not exist in the INS system, although presently it is calibrated against the dry-combustion method. At present, the MDL of the INS system at the 3σ (99%) confidence level and 30-min counting time is about 0.004 to 0.008 g C cm^{-3}. This limit can be further reduced by either counting longer or increasing the number of detectors.

We verified the linearity of the system, although with a limited number of points, at three places: in a sand pit, in the Brookhaven forests, and in Duke Forest. The corrections for interferences in the C peak resulted, however, in overcorrecting the C net peak (a negative intercept in the calibration lines in Fig. 5, 7, and 8). We suspect that the theoretical cascade factor might be too high and it is being investigated at present. Linearity remained when the jack-knifing method was applied to all nine points in the Duke Forest, and the resulting regression was very close to the identity line shown in Fig. 9. This finding is in contrast to those from infrared spectroscopy wherein the calibration line is not linear, indicating lack of specificity. In addition, the INS linearity was also demonstrated by the excellent concordance realized when comparing the Monte Carlo solution of the system model (in Eq. [7]) with the experimental calibration in the sand pit. Once completed and validated, the model in Eq. [7] can be used to create independent calibrations for a variety of soils and conditions, thus bypassing the need for cross-calibration. Using this model, we also calculated that 90% of the signal is generated from an approximate soil volume of 0.3 m^3 reaching a depth of about 30 cm. This is a very large volume, equivalent to averaging or compositing many soil cores (data not shown). This result also demonstrates that there are clear advantages in using the INS system to assess very large areas in contrast to infrared and LIBS methodologies that sample volumes <1 cm^3.

Table 6. Depth profile coefficients (standard errors in parentheses).

Site	*a*	*b*	*c*	Integral (0–30 cm)	Measured
	g C cm^{-3}		cm^{-1}	g C cm^{-2}	
Brookhaven	0.010 (0.002)	0.104 (0.021)	0.187 (0.043)	0.854	0.807
Duke	0.007 (0.002)	0.034 (0.004)	0.114 (0.031)	0.498	0.473

SUMMARY

We demonstrated the feasibility and proof-of-principle of the INS method to nondestructively measure C in soil. It is a multielemental analysis system that can be used in static and scanning modes (not shown here) across arbitrarily large areas, sampling large volumes. It is nondestructive, thus allowing sequential measurements. Continuous improvements in the system prevented systematic errors and gave reproducible measurements. With the implementation of our beta prototype system with 16 detectors, we will enter Phase II of large-scale validation and confirmation. At that stage, many of the outstanding issues will be explored, e.g., universality of the calibration line for various soil types, confirma-

tion of the footprint and volume measured by the instrument, and evaluation of the minimum detectable change in soil C, which differs from the MDL. This new approach also implies revising the conventional wisdom about sampling large areas.

ACKNOWLEDGMENTS

Special thanks to Dr. M. Herman for his helpful discussions of the nuclear data for silicone. The partial support by the U.S. Department of Energy under Contract no. DE-AC02-98CH10886 is recognized.

REFERENCES

Alfassi, Z.B., and C. Chung. 1995. Prompt gamma neutron activation analysis. CRC Press, Boca Raton, FL.

Bhatti, J.S., R. Lal, M.J. Apps, and M.A. Price. 2006. Climate change and managed ecosystems. CRC Press, Boca Raton, FL.

Chang, C.W., D.A. Laird, M.J. Mausbach, and C.R. Hurburgh, Jr. 2001. Near-infrared reflectance spectroscopy: Principal component regression analysis of soil properties. Soil Sci. Soc. Am. J. 65:480–490.

Chrien, R.E., and W.R. Kane. 1979. Neutron capture gamma-ray spectroscopy. Plenum Press, New York.

Climate Change Science Program. 2003. Strategic Plan For the U.S. Climate Change Science Program. U.S. Climate Change Science Program, Washington, DC.

Cramers, D.A., M.H. Ebinger, D.D. Breshears, P.J. Unkefer, S.A. Kammerdiener, M.J. Ferris, K.M. Catlett, and J.R. Brown. 2001. Measuring total soil carbon with laser-induced breakdown spectroscopy (LIBS). J. Environ. Qual. 30:2202–2206.

Csikai, J. 1987. CRC handbook of fast neutron generators. CRC Press, Boca Raton, FL.

Curtis, P.S., P.J. Hanson, P. Bolstad, C. Barford, J.C. Randolph, H.P. Schmid, and K.B. Wilson. 2002. Biometric and eddy-covariance based estimates of annual carbon storage in five eastern North American deciduous forests. Agric. For. Meteorol. 113: 3–19.

Dane, J.H., and G.C. Topp. 2002. Methods of soil analysis. Part 4. Physical methods. SSSA Book Ser. 5. SSSA, Madison, WI.

Ebinger, M.H., M.L. Norfleet, D.D. Breshears, A.D. Cremers, M.J. Ferris, J.P. Unkefer, M.S. Lamb, K.L. Goddard, and C.W. Meyer. 2003. Extending the applicability of laser-induced breakdown spectroscopy for total soil carbon measurement. Soil Sci. Soc. Am. J. 67:1616–1619.

Ehsani, M.R., S.K. Upadhyaya, D. Slaughter, S. Shaffi, and M. Pelletier. 1999. A NIR technique for rapid determination of soil mineral nitrogen. Precis. Agric. 1:217–234.

Evans, R.D. 1955. The atomic nucleus. McGraw-Hill Book Co., New York.

Evans, R.J., T.A. Milne, and M.N. Soltys. 1984. Molecular-beam sampling/mass spectrometric studies of the primary pyrolysis mechanisms of biomass, fossil organic matter, and synthetic polymers. Prepr. Pap. Am. Chem. Soc. Div. Fuel Chem. 29:20–31.

Frolking, S., M.L. Goulden, S.C. Wofsy, S.M. Fan, D.J. Sutton, J.M. Munger, et al. 1996. Temporal variability in the carbon balance of a spruce/moss boreal forest. Global Change Biol. 2:343–366.

Fystro, G. 2002. The prediction of C and N content and their potential mineralization in heterogeneous soil samples using Vis-NIR spectroscopy and comparative methods. Plant Soil 246:139–149.

Goulden, M.L., J.W. Munger, S.M. Fan, B.C. Daube, and S.C. Wofsy. 1996. Exchange of carbon dioxide by a deciduous forest: Response to interannual climate variability. Science 271:1576–1578.

Hasselmann, K. 1997. Are we seeing climate change? Science 276:914–916.

Herman, M., R. Capote, B.V. Carlson, P. Obložinský, M. Sin, A. Trkov, H. Wienko, and V. Zerkin. 2007. EMPIRE: Nuclear reaction model code system for data evaluation. Nucl. Data Sheets 108:2655–2715.

Johnston, C.A., P. Groffman, D.D. Breshears, Z.G. Cardon, W. Currie, W. Emanuel, et al. 2004. Carbon cycling in soil. Front. Ecol. Environ. 2:522–528.

Kincade, K. 2003. LIBS leaves the lab for field work in industry and defense. Laser Focus World 39:71–80.

Lal, R., M. Griffin, J. Apt, L. Lave, and M.G. Morgan. 2004. Managing soil carbon. Science 304:393–394.

Lal, R., J.M. Kimble, and R.F. Follett. 1998. Pedospheric processes and the carbon cycle. p. 1–8. *In* R. Lal et al. (ed.) Soil processes and the carbon cycle. Adv. Soil Sci. CRC Press.

Magrini, K., C. Evans, C. Hoover, C. Elam, and M. Davis. 2002. Use of pyrolysis molecular beam mass spectrometry to characterize forest soil carbon: Method and preliminary results. Environ. Pollut. 116:S255–S268.

McCarty, G.W., J.B. Reeves III, V.B. Reeves, R.F. Follett, and J.M. Kimble. 2002. Mid-infrared and near-infrared diffuse reflectance spectroscopy for soil carbon measurement. Soil Sci. Soc. Am. J. 66:640–646.

Mitra, S., and L. Wielopolski. 2005. Optimizing the gate-pulse width for fast neutron induced gamma-ray spectroscopy. Proc. SPIE 5923:592308, doi:10.1117/12.614569.

Mouget, Y., P. Gosselin, M. Tourigny, and S. Bechard. 2003. Three-dimensional analyses of tablet content and film coating uniformity by laser-induced breakdown spectroscopy (LIBS). Am. Lab. 35(4):20–22.

Nargolwalla, S.S., and E.P. Przybylowicz. 1973. Activation analysis with neutron generators. John Wiley & Sons, New York.

Reeves, J.B., G.W. McCarty, and J.J. Meisinger. 1999. Near infrared reflectance spectroscopy for the analysis of agricultural soils. J. Near Infrared Spectrosc. 9:25–34.

Shepherd, K.D., and M.G. Walsh. 2002. Development of reflectance spectral libraries for characterization of soil properties. Soil Sci. Soc. Am. J. 66:988–998.

Stoy, P.C., G.G. Katul, M.B.S. Siqueria, J.-Y. Juang, K.A. Novick, H.R. McCarthy, A.C. Oishi, J.M. Uebelherr, H.-S. Kim, and R. Oren. 2006. Separating the effects of climate and vegetation on evapotranspiration along a successional chronosequence in the southeastern US. Global Change Biol. 12:2115–2135

United Nations Environment Programme. 2003. How will global warming affect my world? A simplified guide to the IPCC's "Climate change 2001: Impacts, adaptation and vulnerability". UNEP, Geneva.

Viscarra Rossel, R.A., D.J.J. Walvoort, A.B. McBratney, L.J. Janik, and J.O. Skjemstad. 2005. Visible, near infrared, mid infrared or combined diffused reflectance spectroscopy for simultaneous assessment of various soil properties. Geoderma 131:59–75.

Wielopolski, L. 2006. Emerging Modalities for Soil Carbon Analysis: Sampling Statistics and Economics Workshop, Upton, NY. 18–20 Jan. 2006. Workshop summary. BNL Rep. 75762-2006. Brookhaven Natl. Lab., Upton, NY.

Wielopolski, L., S. Mitra, G. Hendrey, I. Orion, S. Prior, H. Rogers, B. Runion, and A. Torbert. 2004. Non-destructive soil carbon analyzer (ND-SCA). BNL Rep.72200-2004. Brookhaven Natl. Lab., Upton, NY.

Wielopolski, L., I. Orion, G. Hendrey, and H. Rogers. 2000. Soil carbon measurements using inelastic neutron scattering. IEEE Trans. Nucl. Sci. 47:914–917.

Wielopolski, L., Z. Song, I. Orion, A.L. Hanson, and G. Hendrey. 2005. Basic considerations for Monte Carlo calculations in soil. Appl. Radiat. Isot. 62:97–107.

Wofsy, S.C. and R.C. Harriss. 2002. The North American Carbon Program (NACP). Report of the NACP Committee of the U.S. Carbon Cycle Science Program. U.S. Global Change Research Program, Washington, DC.